



Electrical characterization of thermoelectric generators based on p-type $\text{Bi}_{0.4}\text{Sb}_{1.6}\text{Se}_{2.4}\text{Te}_{0.6}$ and n-type $\text{Bi}_2\text{Se}_{0.6}\text{Te}_{2.4}$ bulk thermoelectric materials

A. Kadhim^{a,b,*}, A. Hmood^{a,b}, H. Abu Hassan^a

^a School of Physics, Universiti Sains Malaysia, 11800 (USM), Penang, Malaysia

^b Department of physics, College of science, University of Basrah, Basrah, Iraq

ARTICLE INFO

Article history:

Received 10 September 2012

Accepted 12 January 2013

Available online 1 February 2013

Keywords:

Contacts

Semiconductors

Powder technology

Solidification

ABSTRACT

In this study, we fabricated two thermoelectric (TE) generation (TEG) devices based on p- $\text{Bi}_{0.4}\text{Sb}_{1.6}\text{Se}_{2.4}\text{Te}_{0.6}$ and n- $\text{Bi}_2\text{Se}_{0.6}\text{Te}_{2.4}$ bulk TE materials. The overall dimensions of these devices, which comprise 9 (D_1)- and 18 (D_2)-couples of legs connected and attached to alumina substrates by Ag paste–Cu plate–Ag paste electrodes, are 50 mm × 25 mm and 50 mm × 50 mm, respectively. The open-circuit voltage (V_{oc}) and the maximum output power (P_{max}) were estimated in terms of the temperature difference (ΔT) between hot (T_H) and cold (T_C) junctions as well as the number of p–n couples of the TEG devices. The significance of the resistances, including the internal resistance (R_{in}) and contact resistance (R_c) between legs and electrodes, are discussed. P_{max} obtained with the D_2 device was 273 mW under thermal conditions of $T_H=523$ K and $\Delta T=184$ K.

© 2013 Elsevier B.V. All rights reserved.

1. Introduction

A thermoelectric (TE) power generation (TEG) device produces voltage when a temperature difference (ΔT) exists between the hot and the cold sides of the device because of the Seebeck TE effect [1]. These generators have the following advantages: no moving parts, small and lightweight, maintenance-free, acoustically silent and electrically “quiet,” and environmentally friendly [2]. Bi_2Te_3 -based chalcogenides have attracted considerable interest for their promising TE properties [3]. However, the enhancement of TE properties is strongly required for empirical applications. An approach for the enhancement of TE properties is the optimization of the doping effective route. For example, recent devices have used Bi_2Te_3 , a semiconductor that, when alloyed with antimony (Sb) or selenium (Se), becomes an efficient TE material for power generation because of the variations in carrier concentration and carrier mobility [4,5]. As an alternate approach, researchers have attempted to improve the efficiency of materials based on Bi_2Te_3 by creating structures with one or more reduced dimensions [6]. In one case, an n-type Bi_2Te_3 has been shown to have an improved Seebeck coefficient (S). However, S and electrical conductivity (σ) have a trade-off; a higher S results in decreased carrier concentrations and decreased σ [7]. The fundamental physical parameters of Bi–Sb–Se–Te and Bi–Se–Te TE materials such as σ , S , and power factor (P_{factor}) are given in our

previous papers [8,9], which reported that the highest P_{factor} has been obtained for compositions of $\text{Bi}_{0.4}\text{Sb}_{1.6}\text{Se}_{2.4}\text{Te}_{0.6}$ and $\text{Bi}_2\text{Se}_{0.6}\text{Te}_{2.4}$. For $\text{Bi}_2\text{Se}_{0.6}\text{Te}_{2.4}$ as n-type materials, the carrier concentration is adjusted by doping with tellurium (Te), which is conducted in the present paper. Te atoms exhibit a donor action because they replace Se atoms in the lattice, each contributing one electron to the conduction band [10]. Apparently, the ionization energy of a Te atom is very low. Therefore, this atom in $\text{Bi}_2\text{Se}_{0.6}\text{Te}_{2.4}$ is almost fully ionized. As an extension of our previous work, we fabricated 9 and 18 couples of TEG devices and focused on the properties of the two devices that use $\text{Bi}_{0.4}\text{Sb}_{1.6}\text{Se}_{2.4}\text{Te}_{0.6}$ as p-type and $\text{Bi}_2\text{Se}_{0.6}\text{Te}_{2.4}$ as n-type materials.

2. Experimental procedure

The p-type and n-type ingots were grown using solid-state microwave synthesis, as described in previous literature [8,3]. After grinding the ingots, both types of powders were pressed into disks (5 mm in diameter and 3.5 mm thick) through cold pressing at 10 t. The assemblies of 9 (D_1) and 18 (D_2) couples from these pellets were placed between two alumina plates with the corresponding dimensions of 50 mm × 25 mm and 50 mm × 50 mm, respectively, which served as hot and cold ends for the relevant TE pellets. The electrodes for TEG device should have high thermal conductivity in the thickness direction and high electrical conductivity in the plane direction [11]. Therefore, Ag paste–Cu plate–Ag paste electrodes were employed and designed because Cu has the highest thermal conductivity and electrical conductivity among all metals. The Ag paste–Cu plates–Ag paste electrodes

* Corresponding author at: School of Physics, Universiti Sains Malaysia, 11800 (USM), Penang, Malaysia. Tel.: 60174519357; fax: 6046579150.

E-mail address: areejkadhim@yahoo.com (A. Kadhim).

were prepared on the inner surface of the alumina substrates. The devices were then dried at room temperature for one day to metalize the electrodes on the devices. Selected regions of the electrodes were imaged using scanning electron microscope (SEM; JSM-6460). To evaluate device performance, the top alumina plate was heated up to 523 K using one brass block as a heater for the device, and the bottom plate was cooled by another brass block with circulated cooling water. ΔT between the hot and the cold sides was measured by two digital K-type E[®] Sun (ECS820C) thermocouples near the inner surface of the alumina substrates. The current–voltage (I – V) lines and the current–power (I – P) curves of power generation were measured in air using variable load resistance (R_L) and a Keithley 197 voltmeter.

Reproducibility measures how closely two or more measurements agree one another [12]. Given that the number of parts (n)=5, number of trials (r)=2, and number of appraisers=3, $\text{Reproducibility} = \sqrt{(2.696\bar{X})^2 - (\text{Repeatability}^2/nr)}$, where \bar{X} is the average of the difference in the average measurements between the appraiser with the highest average measurements and the appraiser with the lowest average measurements for all appraisers and parts. $\text{Repeatability} = 4.478\bar{R}$, where \bar{R} is the average of the ranges for all appraisers and parts.

3. Results and discussion

The output voltage (V_{out}) and the output power (P_{out}) of the fabricated 9(D_1)- and 18 (D_2)- couples versus the current (I_{out}) were measured by sweeping R_L at several temperature conditions, as shown in Fig. 1(a) and (b). The first study involved the determination of the I – V output characteristic of the TEG devices. As expected, V_{out} increased with the ΔT . The linearity behavior can be seen in all I – V plots and exhibit almost the same slope. This finding indicates that the R_{in} of the TEG devices is almost constant with the ΔT and load operations for each device. From these I – V output characteristics, we can obtain the R_{in} of the device. The V_{oc} that is equal to the intercept of the I – V line reached 586 mV and 1480 mV for D_1 and D_2 , respectively, at ΔT of 184 K and T_H of 523 K, which are in agreement with the expression $V = V_{oc} - R_L I$. This value is lower than that calculated based on the S – T curves [8,3] of both p- and n-type legs ($V_{\text{calculated}} = (S_p - S_n) \times \Delta T \times N$, where N is the number of couples). This voltage loss could have originated from numerous factors including low thermal conductivity of alumina substrate [13] and unfavorable junctions between the TE legs and the electrodes. The main factors responsible for the unfavorable junctions could be attributed to dry joints, including some pores, originating from the differences between the legs and the electrodes in terms of thermal expansion and/or poor affinity. The I – P curves illustrated in Fig. 1(a) and (b) exhibit the parabolic curves of the P_{out} ; an analysis of the plots of I – V lines enable the observation of an increase in P_{out} with ΔT . This observation results from the rise of the ΔT , the consequence of which is an increase in V_{oc} (Table 1). A higher value of V_{oc} results in a higher I_{out} for a given R_L , thus becoming the dissipated power in the external load ($P_{out} = R_L I_{out}$). The maximum output power P_{max} values were 88.5 and 273 mW for D_1 and D_2 , respectively, at the thermal condition of 523 K T_H and $\Delta T = 184$ K, which suggests these results are comparable with the results of Shanyu et al. [4]. The powers of devices that were improved by increasing the number of couples between the hot and the cold sides were investigated. V_{oc} and P_{max} systematically increased with the number of p–n couples, thus indicating that TE power could be simply controlled by a change in module design. The R_{in} of each device, which corresponds to the slope of the I – V lines, was directly obtained by the measured system. The R_{in} of the TEG

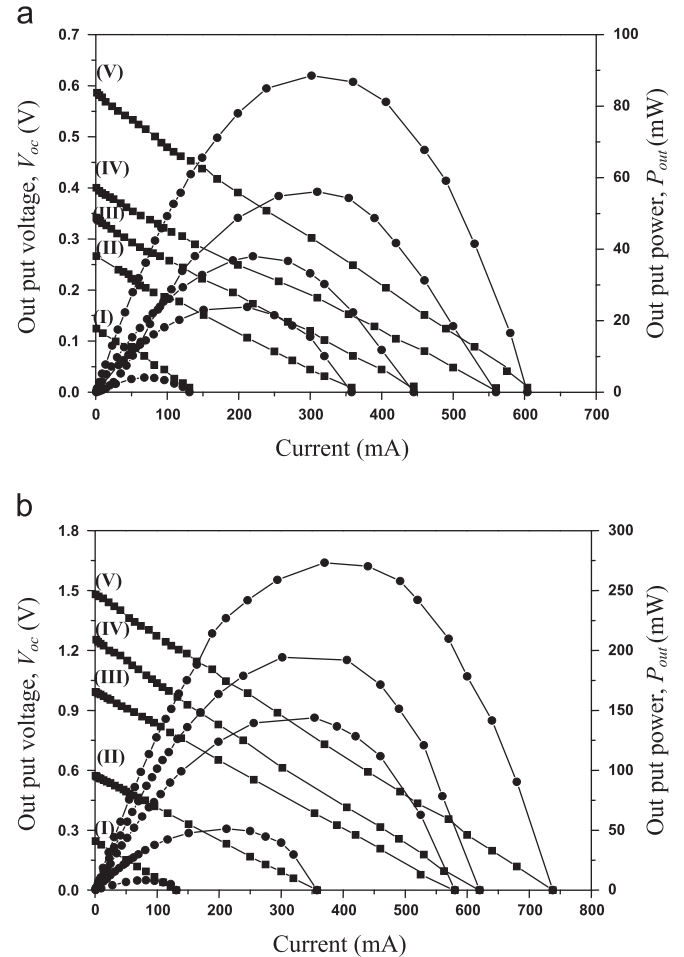


Fig. 1. Output voltage (V_{out}) and output power (P_{max}) as a function of electric current of the TEG device comprising (a) 9 (D_1) and (b) 18 (D_2) couples, respectively, where (I) $\Delta T=27$, (II) $\Delta T=66$, (III) $\Delta T=104$, (IV) $\Delta T=145$, and (V) $\Delta T=184$ K.

Table 1

Maximum open-circuit voltage (V_{oc}) and output power (P_{max}) under various ΔT for D_1 and D_2 .

D	ΔT (K)	27	66	104	145	184*
1	V_{oc} (mV)	124	266	342	400	586
	P_{max} (mW)	4.10	23.8	38.0	56.1	88.5
2	V_{oc} (mV)	246	572	992	1253	1480
	P_{max} (mW)	8.34	51.2	144	194	273

* Reproducibility at $T_H=523$ K and $\Delta T=184$ for D_1 and D_2 are 14.14 and 15.75, respectively.

device comprises the ideal internal resistance (R_{id}) (the resistance values of p- and n-type samples) and the electrical contact resistance R_c ($R_c = R_{in} - R_{id}$ [2]), which in turn includes the resistance of the electrodes (Ag paste–Cu plate–Ag paste) and the boundary resistance between the electrodes and the thermoelectric legs [14]. In these generators, R_c is mostly attributed to the boundary resistance because the resistance of Ag–Cu–Ag electrodes is known to be very small [2]. The resistance values of D_2 ($R_{in}=2.01 \Omega$ and $R_c=1.57 \Omega$) were two times larger than those of D_1 ($R_{in}=0.97 \Omega$ and $R_c=0.75 \Omega$), which could be attributed to the differences in size and electrode contact areas among the two devices [15]. Therefore, we consider that the increase in R_c might be attributed to the boundary resistance between the electrodes and thermoelectric legs. Fig. 2 presents

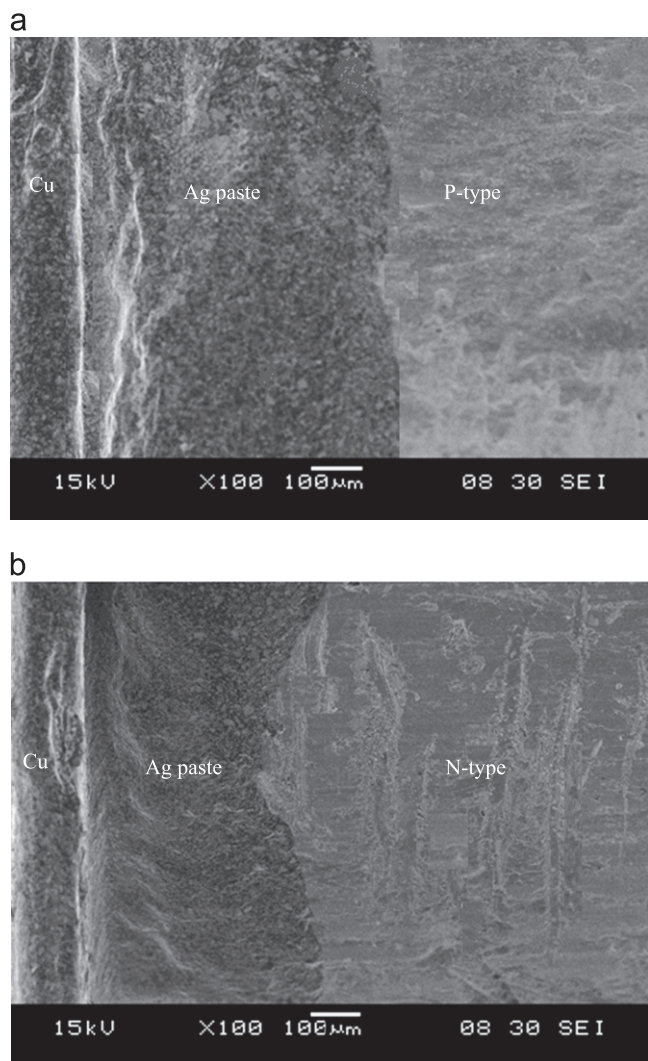


Fig. 2. SEM images at the junction of (a) p-type $\text{Bi}_{0.4}\text{Sb}_{1.6}\text{Se}_{2.4}\text{Te}_{0.6}$ leg and (b) n-type $\text{Bi}_2\text{Se}_{0.6}\text{Te}_{2.4}$ leg.

the SEM images of junctions of p-type $\text{Bi}_{0.4}\text{Sb}_{1.6}\text{Se}_{2.4}\text{Te}_{0.6}$ and n-type $\text{Bi}_2\text{Se}_{0.6}\text{Te}_{2.4}$ legs. These junctions demonstrate that, with the relationship between R_c and P_{max} , R_c should be minimized for each device because of its key role in TEG device performance.

4. Conclusions

Chalcogen-based TEG devices were fabricated using $\text{Bi}_{0.4}\text{Sb}_{1.6}\text{Se}_{2.4}\text{Te}_{0.6}$ and $\text{Bi}_2\text{Se}_{0.6}\text{Te}_{2.4}$ bulk TE materials as the p- and n-legs, respectively. The 9- and 18-couple TE devices were successfully prepared and characterized in terms of P_{max} and high V_{oc} . The 18-couple device could generate up to 273 mW, which is larger than that of the 9-couple device under the thermal conditions $T_H=523$ K hot side temperature and $\Delta T=184$ K temperature difference. The special design of the electrode structure of the Ag paste–Cu plate–Ag paste is demonstrated to be an effective for enhancing device performance. The successful demonstration of the excellent TE performances of the as-prepared devices suggests the great potential of these p- $\text{Bi}_{0.4}\text{Sb}_{1.6}\text{Se}_{2.4}\text{Te}_{0.6}$ and n- $\text{Bi}_2\text{Se}_{0.6}\text{Te}_{2.4}$ TE materials for future power generation applications.

Acknowledgments

This work was entirely supported by the PRGS Grant no.1001/PFIZIK/844091 of USM.

References

- [1] Gaowei L, Jiemin Z, Xuezhong H. Appl Energy 2011;88:5193–9.
- [2] Ling H, Yang J, Shanying L, Huangming S, Xinzhen L, Kaixuan Q, et al. J Alloys Compd 2011;509:8970–7.
- [3] Kadhim A, Hmood A, Abu Hassan H. Mater Lett 2011;65:3105–8.
- [4] Shanyu W, Wenjie X, Han L, Xinfeng T. Intermetallics 2011;19:1024–31.
- [5] Kadhim A, Hmood A, Abu Hassan H. Mater Sci Semicond Process 2012;15:549–54.
- [6] Joohoon K, Jin-Seo N, Wooyoung L. Nanoscale Res Lett 2011;6:277.
- [7] Yoo BY, Huang C-K, Lim JR, Herman J, Ryan MA, Fleuriel J-P, et al. Electrochim Acta 2005;50:4371–7.
- [8] Kadhim A, Hmood A, Abu Hassan H. Mater Lett 2012;81:31–3.
- [9] Kadhim A, Hmood A, Abu Hassan H. Adv Mater Res 2012;501:126–8.
- [10] Rowe DM. Thermoelectrics handbook: macro to nano. USA: CRC Press Taylor & Francis Group; 2006.
- [11] Sui T, Li J-F, Jin S. Joining CoSb_3 to Metal Surface of FGM Electrode for Thermoelectric Modules by SPS. Key Eng Mater 2008;368–372:1858–61.
- [12] Taylor JR. An introduction to error analysis: the study of uncertainties in physical measurements. 2d Edition USA: University Science Books; 1997.
- [13] Degang Z, Changwen T, Shouqiu T, Yunteng L, Likun J, Lidong C. Mater Sci Semicond Process 2010;13:221–4.
- [14] Takashiri M, Shirakawa T, Miyazaki K, Tsukamoto H. Sensors and Actuators A 2007;138:329–34.
- [15] Woosuk S, Norimitsu M, Koichiro I. J Power Sources 2011;103:80–5.